SECED 2023 Conference
Earthquake Engineering & Dynamics for a Sustainable Future
14-15 September 2023, Cambridge, UK

INFLUENCE OF STRONG MOTION AND SYSTEM CHARACTERISTICS ON THE BEHAVIOUR OF INTEGRATED DAMPING TECHNIQUES

Romeo CUKA[1], Miguel MARTINEZ-PANEDA[2] & Ahmed Y. ELGHAZOULI[3]

Abstract: *Tall buildings are experiencing unparallel growth in response to denser and more populated cities. Beyond conventional design approaches, based on providing strength and stiffness, state-of-the-art designs aim to incorporate damping systems to reduce the large carbon footprint associated with high-rise construction. Towards this aim, this research focuses on a recently proposed damping system capable of mobilizing a large part of the building as a damper mass. The system generates damping through the differential motion between a movable mass and the main frame and connects it via springs in parallel with fluid viscous dampers. The springs control the static displacements between the damper mass and the rest of the building. The fluid viscous dampers dissipate energy and control accelerations. While previous research has considered the fluid viscous damper behaviour, the spring characteristics and contributions have not been examined. The spring stiffness defines the level of differential displacement between the core and the movable mass and hence is recognized to play a major role in the response of the system. In this study, the optimum vertical distribution through the movable floors is first investigated under five deterministic and sequential arrangements and assessed for the level of additional equivalent damping. These distributions are then evaluated through four key performance indexes under selected far-field, near-field, and pulse-like real earthquake excitations. Findings from the assessments shed light on the benefits of alternative spring distributions for large mass damper arrangements, and the significantly different performance between conventional tuned mass dampers and large mass dampers when accounting for different earthquake excitations. The introduction of such damping techniques is shown to bring significant benefits in reducing the carbon footprint of tall buildings and contribute towards the path for sustainable infrastructure.*

Introduction

Construction of tall and mega-tall buildings has been experiencing a drastic rise in recent decades, particularly in areas of high-density or large economic growth. As buildings get taller, wind forces start to have a more present role in the design and their induced displacements and accelerations can become the governing criteria driving structural efficiency. The design should satisfy both life safety ultimate limit state and wind-induced acceleration limits. An efficient way to control wind-induced accelerations and seismic forces is through the implementation of a supplementary damping system (Smith & Willford, 2007). Cost savings from the implementation of supplementary damping systems are widely reported, such as for 250 West 55th Street in NY, where the incorporation of a Damped Outrigger system led to savings of approximately 1,000 tons of steel (Jackson & Scott, 2012). Tall buildings designed with a supplementary damping system can achieve a more resilient and efficient design by behaving essentially elastic under frequent earthquakes and only experiencing relatively low damage, compared to their undamped counterparts, under severe earthquakes. Energy is dissipated through the damping system rather than through inelastic behaviour or damage.

Different well-established supplementary damping systems include metallic yield dampers (Perry et al, 1993), friction dampers (Pall & Marsh, 1982), viscoelastic dampers (Chang et al, 1995), fluid viscous dampers (Constantinou & Symans, 1993) with variations such as that of the Damped Outrigger (Smith & Willford, 2007), or the arguably most used Tuned Mass Damper (TMD) (Connor, 2003). TMDs are formed by an added mass, typically 0.5 to 1% of the total of the building, a spring, and a damper working together to dissipate energy by the inertia force of the

[1] Imperial College London, London, UK, r.cuka@hotmail.com
[2] Senior Structural Engineer, Arup, London, UK
[3] Professor, Imperial College London, London, UK

tuned mass acting in the opposite direction of the induced forces. Since its first application in the Boston John Hancock building in 1976, it has been widely applied throughout the world (Gutierrez, Soto & Adeli, 2013) due to its good performance and simplicity despite its several limitations. A mass damper can only be tuned in one frequency, hence the efficiency of the damper decreases, especially in tall buildings where higher modes can be significant. This limitation could be alleviated by increasing the size of the TMD and mobilizing a larger mass ratio (Rana & Soong, 1998). Alternative variations include multiple-tuned mass dampers (MTMD), which, although does not improve the system efficiency, have the potential to be more robust than a single TMD and spread over a wider frequency range (Xu & Igusa, 1992). Another major drawback is the TMD's inability to mitigate pulse excitations, as they cannot reach a resonant response at peak. Another disadvantage is that the TMD is placed at the top of the building, a position which maximizes its efficiency, yet leads to a significant loss of valuable space. A variation to overcome this is the idea of placing a heavy garden at the roof level acting also as a TMD (Matta & De Stefano, 2009). To mitigate conventional TMD's limitations, several research studies have investigated the benefit of using active or hybrid systems. Active control systems are however associated with a higher cost and complexity, with a potentially reduced reliability due to their dependency on the power supply that may not be present during severe seismic excitations (Soong & Spencer, 2002).

A novel mass damping system referred to as the Integrated Damping System (IDS) was recently introduced based on the basic concept of conventional tuned mass damper notion yet with the aim of overcoming most of its deficiencies (Martinez-Paneda & Elghazouli, 2020). The IDS approach aims to mobilize a large portion of the building's own mass as damper mass and generate damping by controlling the differential motion between the movable part and the rest of the building. IDS consists of a damper and a spring in parallel, which connects the lateral load-resisting system of the building with the movable floors.

The primary purpose of this study is to investigate the behaviour of a structure incorporating IDS while using different spring distribution arrangements along the height of the movable mass. Research (Xu & Igusa, 1992) have shown that not only an increased mass ratio can lead to increased equivalent damping, but it can also reduce the relative movement between the damped mass and the building, for specified equivalent damping. Detuning is also significantly reduced when the mass ratio is relatively large for both main mass and ground excitation (Martinez-Paneda & Elghazouli, 2022). Wind-induced accelerations in the movable portion of the building are controlled by fluid viscous dampers (FVD), placed between the moving mass and the rest of the building. As fluid viscous dampers lack static stiffness, a spring is placed in parallel to resist the mean static component of the wind forces. Although previous research efforts have looked at the characterization and behaviour of the FVD along the height over which the IDS spans (Martinez-Paneda & Elghazouli, 2021), no study has yet focused on the spring contribution. This is especially important as the spring is the key element defining the level of differential displacement and hence the level of additional equivalent damping that can be generated. This paper investigates the behaviour of the springs and their characterization by assessing their response through a series of key performance indexes for different heuristic and analytical vertical distributions in an illustrative 300 m tall building, hence providing insight into the performance of the system. System characterization is further investigated by assessing the benefits and performance of a selection of real far-field, near-field, and pulse-like seismic excitations.

Structural model

The present study is performed by investigating the system response in an illustrative 300 m tall building employed by Martinez-Paneda & Elghazouli (2021) in a previous study to assess the response and contribution of FVDs. The lateral stability system is a 20 m x 20 m steel braced core made from Concrete-Filled Steel Tube (CFT) columns centred on a 54 m x 54 m square plan (Figure 1). Perimeter columns are standard CFT sections tapering to match the axial demands. The structure comprises 65 floors with a 4.5 m height per floor and is divided into three tiers, with the ground floor and MEP transition floors designed as 9 m tall. The IDS is implemented in the top tier, corresponding to the top third of the building. Additional details on material properties, element sections, and weights can be found elsewhere (Martinez-Paneda & Elghazouli, 2021). Modal mass participation ratios and fundamental periods for the first six modes are reported in Table 1. The building has a relatively long fundamental period (10 sec) due to the relatively high flexibility. While this might not be acceptable in a conventional design, due to the large added damping, wind-induced accelerations and drifts were shown to be within acceptable limits.

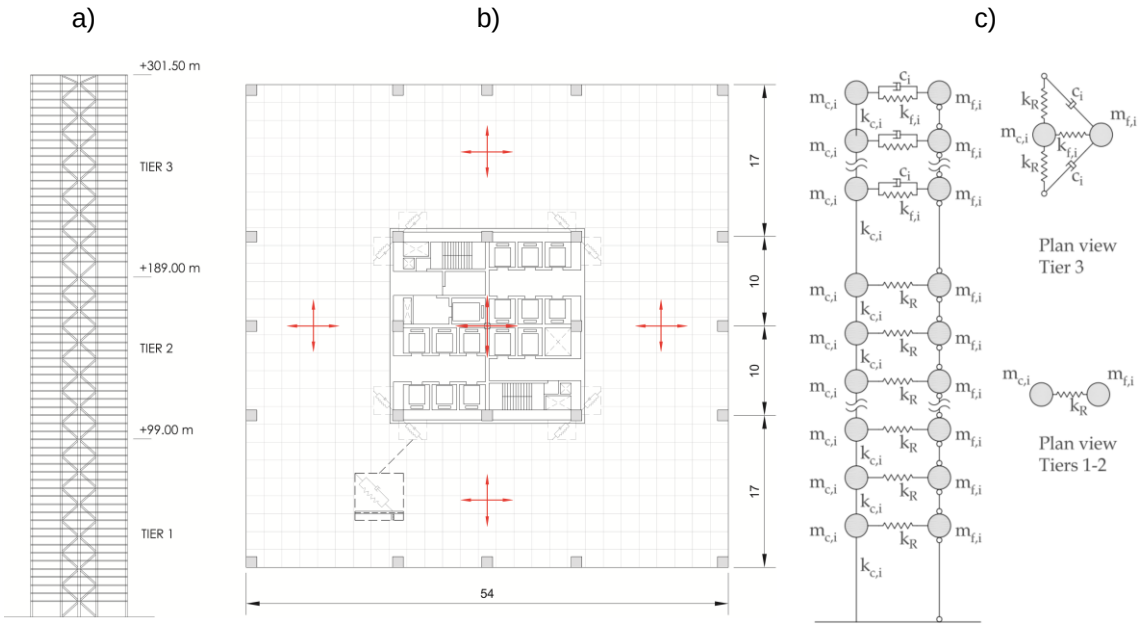

Figure 1: Case study building: a) Elevation view, b) Plan view, and c) simplified model

Mode	Period [s]	UX	UY	RZ
1	*9.9*	*36%*	*23%*	*0%*
2	*9.9*	*23%*	*36%*	*0%*
3	*5.0*	*0%*	*0%*	*77%*
4	*2.4*	*0%*	*21%*	*0%*
5	*2.4*	*21%*	*0%*	*0%*
6	*1.9*	*0%*	*0%*	*12%*

Table 1: Modal mass participation ratios for first 6 modes (Martinez-Paneda & Elghazouli, 2021)

The building response is investigated using a one-directional simplified model as depicted in Figure 1.c. The core and floor masses on every floor are defined as lumped masses at their respective heights and are connected with rigid links at every floor level in the first two tiers. The third tier, where the IDS is located, replaces the rigid link with a spring in parallel with a damper. The dampers on each floor are set in a 45 degrees arrangement to maximise energy dissipation.

The finite element program SAP2000 (CSI, Berkley California, 2021) was used for the analysis. Results were extracted from nonlinear time-history analysis using direct integration with an intrinsic damping ratio of 0.8%. To assess the response of the system and the impact of the spring definition, five spring distributions were generated from heuristic or analytical methods with the same average stiffness. Dampers were defined as linear, with a damper exponent, a, of unity following the Maxwell model (Martinez-Paneda and Elghazouli, 2021). The optimum damper coefficient, c, was calculated for each spring distribution to maximise the additional equivalent damping, ξ, using the half-power bandwidth method (Papagiannopoulos & Hatzigeorgiou, 2011).

Seismic excitations

The response of the model and spring distributions were assessed under three sets of seven ground motion records (Figure 2) obtained from the PEER NGA Database (2005) and representing far-field (with a distance from the fault beyond 200 km), near-field (with a distance from the fault of less than 20 km), and pulse-like records (Cheng & Bai, 2017). The records (Table 2) were chosen to match the EC8 Type 1, Soil C, target spectrum with a PGA of 0.25g (Eurocode 8, 2004), minimising the mean squared error for all but the pulse-like records, MSE, over a period of 2 sec to 10 sec with a scaling factor ranging from 0.2 to 5.0 (Bravo et al., 2020). The records were selected with a magnitude of M 6.5 to 7.3; and a shear wave velocity, V_s, from 180 m/s to 360 m/s.

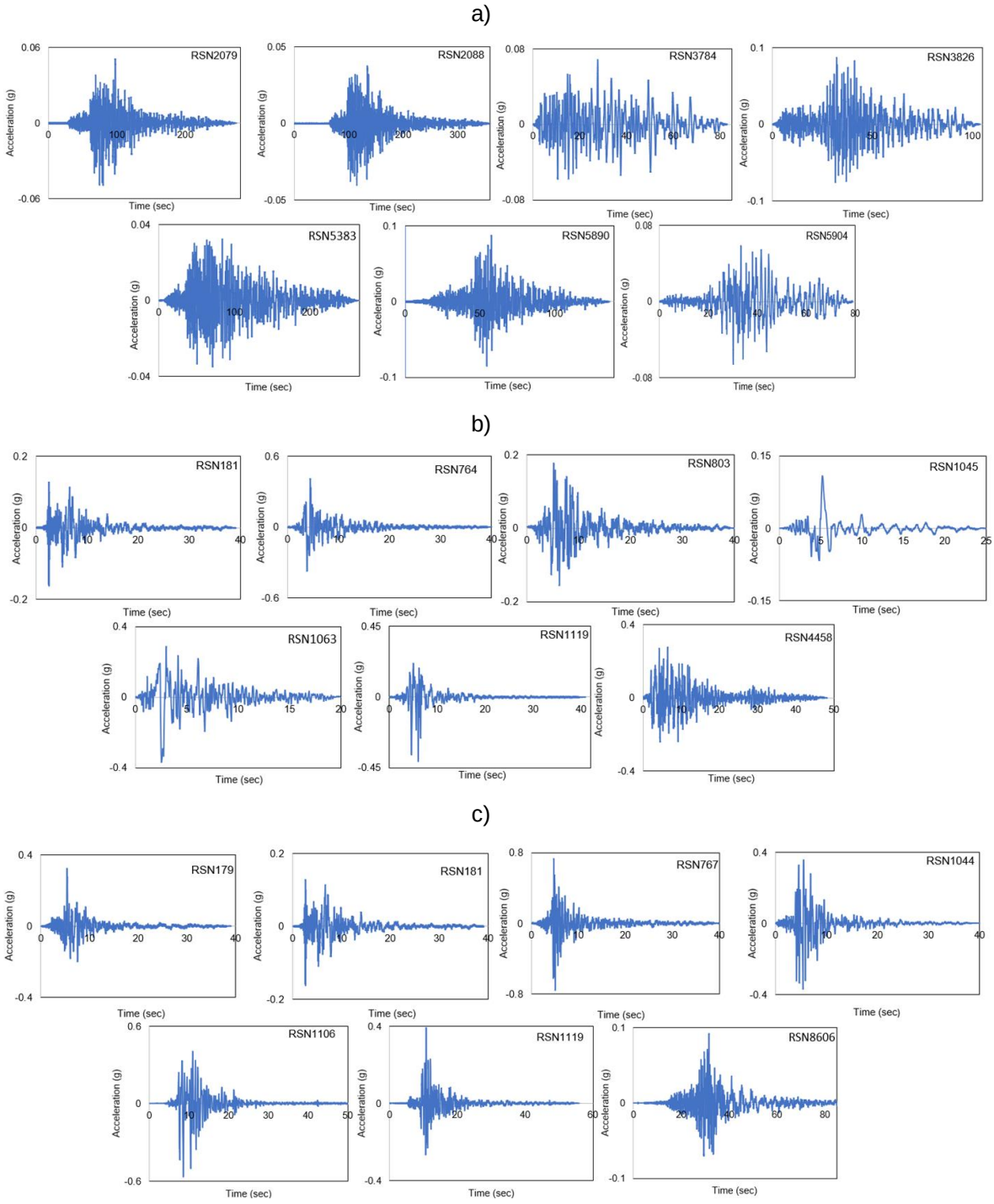

Figure 2: Scaled acceleration time histories for a) the far-field, b) near-field c) pulse-like seismic records

Spring characteristics

Three key spring related parameters can affect the behaviour: (i) the average spring stiffness, which determines the overall level of differential motion and hence has the largest influence on the level of additional damping generated, (ii) the spring response, for either linear or non-linear cases that could allow larger displacements under large seismic events, and (iii) vertical stiffness distribution. The first parameter has the largest effect yet is bounded by detailing and practical limitations and is hence assumed as 150 mm under the static 50-year return period UK-NA static wind load (CEN, 2005) as proposed in previous work (Martinez-Paneda & Elghazouli, 2021). With that 150 mm set as the average stiffness value, five different heuristic and analytical vertical stiffness distributions (Figure 3) are investigated as follows:

- Uniform differential displacement (UDD): This distribution aims to have a uniform differential movement of 150 mm along the height of the third tier under the wind static load as per the UK-NA to Eurocode 1 part 4 (CEN, 2005). Spring stiffness per floor is obtained using Hooke's law for the wind pressure and tributary area of each floor.

Database ID Number	Earthquake Name	Year	Distance from fault (km)	Magnitude (M)	Vs30 (m/sec)	PGA (g)	Scale Factor	MSE
Far-field excitations								
RSN2079	"Nenana Mountain_ Alaska"	2002	271.9	6.7	272	0.05	4.63	0.06
RSN2088	"Nenana Mountain_ Alaska"	2002	272.9	6.7	342	0.04	4.47	0.06
RSN3784	"Hector Mine"	1999	251.5	7.1	351	0.07	3.97	0.07
RSN3826	"Hector Mine"	1999	211.7	7.1	308	0.09	3.16	0.04
RSN5383	"Chuetsu-oki_ Japan"	2007	215.2	6.8	230	0.04	4.23	0.12
RSN5890	"El Mayor-Cucapah_ Mexico"	2010	200.6	7.2	350	0.09	2.65	0.19
RSN5904	"El Mayor-Cucapah_ Mexico"	2010	227.5	7.2	340	0.07	3.61	0.2
Near-field excitations								
RSN181	"Imperial Valley-06"	1979	1.4	6.5	203	0.16	0.36	0.02
RSN764	"Loma Prieta"	1989	11.1	6.9	271	0.41	1.53	0.01
RSN803	"Loma Prieta"	1989	9.3	6.9	348	0.18	0.68	0.02
RSN1045	"Northridge-01"	1994	5.5	6.7	286	0.11	0.26	0.01
RSN1063	"Northridge-01"	1994	6.5	6.7	282	0.37	0.42	0.01
RSN1119	"Kobe_ Japan"	1995	0.3	6.9	312	0.41	0.59	0.03
RSN4458	"Montenegro_ Yugoslavia"	1979	5.8	7.1	319	0.28	0.94	0.02
Pulse-like excitations								
RSN179	"Imperial Valley-06"	1979	7.1	6.5	209	0.32	0.67	*0.18*
RSN181	"Imperial Valley-06"	1979	1.4	6.5	203	0.16	0.36	0.02
RSN767	"Loma Prieta"	1989	12.8	6.9	350	0.76	1.36	0.09
RSN1044	"Northridge-01"	1994	5.9	6.7	269	0.37	0.63	0.02
RSN1106	"Kobe_ Japan"	1995	1.0	6.9	312	0.57	0.68	0.04
RSN1602	"Duzce_ Turkey"	1999	12.0	7.1	294	0.39	0.53	0.03
RSN8606	"El Mayor-Cucapah_ Mexico"	2010	11.4	7.2	242	0.09	0.36	0.6

Table 2: Seismological data and scaling factors for selected records (PEER, NGA Database)

- Uniform stiffness distribution (USD): This spring arrangement is defined by applying the total static wind load uniformly throughout the third tier and distributing the required stiffness evenly between floors. It is included herein due to its practical benefits and simplicity.
- Modal proportional (MP): This arrangement is defined by distributing the total stiffness proportionally to the first mode shape of the core. It is arranged to pivot around the middle of the third tier, where the stiffness is set to match the 150 mm differential displacement.
- Modal inverted proportional (MIP): The total stiffness is distributed in an inversely proportional manner with respect to the first mode shape of the core. This results in an inverted arrangement of the MP with the lower storeys having a higher stiffness value and a more flexible top.
- Simplified sequential search algorithm (SSSA): This is an established method for damper placement optimisation that is based on identifying the locations that experience the largest velocity in a sequential manner (Lopez Garcia, 2001). For this application, the algorithm was used to set the springs stiffnesses to allow a maximum differential displacement of 150 mm, within a +/- 1% range, between the core and the movable mass at every storey under the first mode forced vibration with an amplitude of H/500. This was achieved by defining an automated

procedure to iteratively increase or decrease stiffness, as appropriate, based on the results of the previous analysis until the 1% deviation from the 150mm is met. Although the building is designed to just meet a top deflection of H/500 under the static wind load, the SSSA distribution results in a smaller overall stiffness when compared to the other counterparts and hence generally results in larger differential displacements. To avoid excessively long movements, the maximum differential displacement per floor was capped at double the stiffness corresponding to the 150 mm baseline case within a margin of +/- 5%.

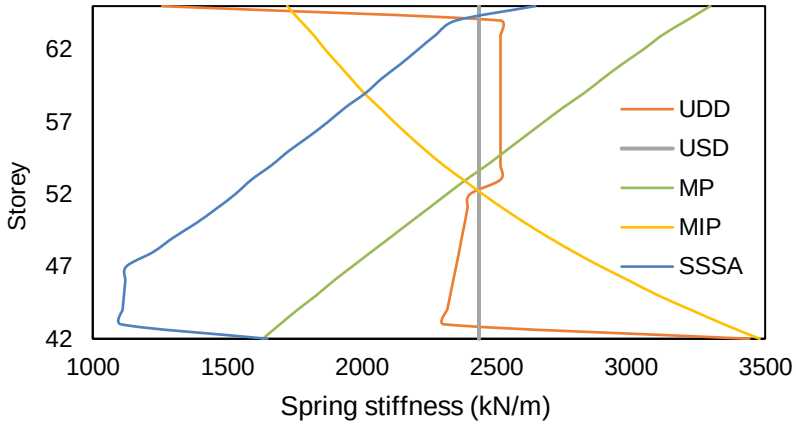

Figure 3: Spring stiffness distribution along the height of the 3rd Tier

Equivalent damping

The defined spring arrangements are assessed in terms of the equivalent damping ξ, using the half-power bandwidth method, as shown in Figure 4. As indicated, the more flexible arrangement SSSA provides the maximum equivalent damping (7.48%). This arrangement also has the maximum average differential displacement over the height, confirming that the more the movable mass is allowed to displace, the more damping is generated.

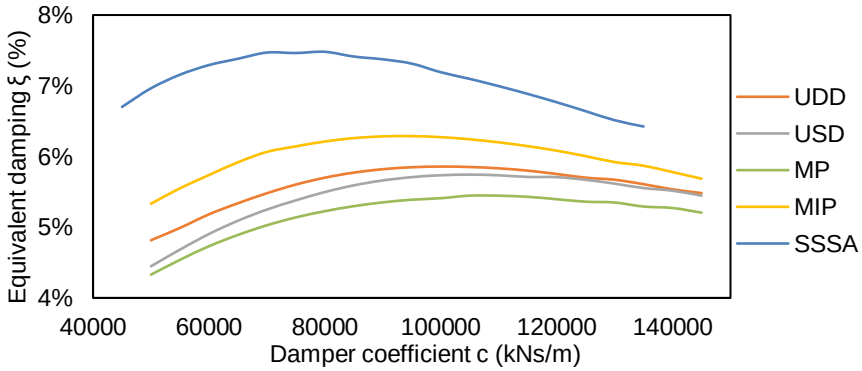

Figure 4: Equivalent damping ξ variation with damper coefficient c for each spring placement

The other four distributions have the same total stiffness, but the equivalent damping ξ varies. The first two distributions UDD and USD, which are directly defined from the UK-NA forces, seem to have nearly the same ξ value of around 5.8%. On the other hand, although the modal proportional (MP) distribution has the same total stiffness, it generates lower damping (5.45%) (Table 4). The opposite occurs with the modal inverted proportional, which provides the largest equivalent damping among the four arrangements (6.29%). It is also more beneficial to release the upper stories by setting lower stiffness than the lower stories of the 3rd Tier.

Spring distributions	UDD	USD	MP	MIP	SSSA
K total (kN/m)	58448	58464	58447	58450	40447
ξ (%)	5.86%	5.74%	5.45%	6.29%	7.48%
c optimum (kNs/m)	100000	105000	105000	95000	80000

Table 4: Total stiffness, equivalent damping ξ, and optimum c for each spring distribution

Seismic response

Far-field records

From the results, it is evident that the building response under far-field excitations can be greatly enhanced with the IDS. For example, considering the top displacement time history for the RSN5904 record for all the spring distributions and the corresponding rigid case (Figure 5). All five spring distributions seem to give similar displacement reductions, with the SSSA producing an average reduction of 43%, partly due to its lower overall stiffness which enhances the system performance, followed by the MIP with a 39% reduction (Table 5). The maximum absolute accelerations for every floor reduce throughout the whole building, but more significantly over the stories in which the IDS is placed (Figure 6.a). Inter-storey drifts are also greatly reduced when compared to the rigid counterpart within a range of 35% to 39% (Figure 6.b).

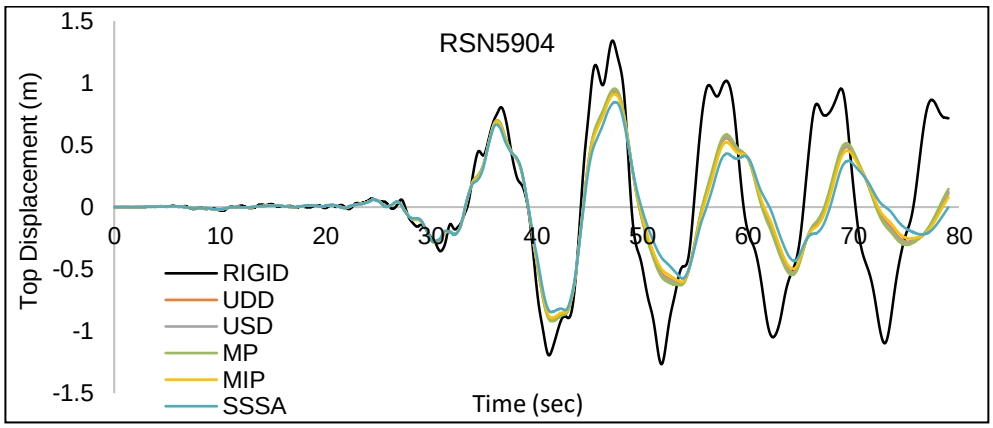

Figure 5: Top displacement for the RSN5904 record for all spring distributions and the rigid case

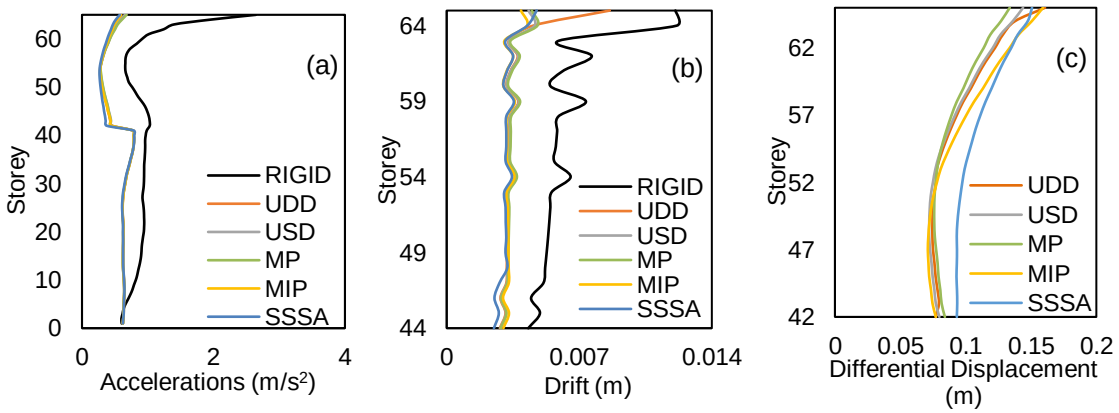

Figure 6: Averaged maximum absolute accelerations (a), averaged maximum inter-storey drifts (b), averaged smaximum differential displacements (c) for far-field seismic records per floor

The SSSA arrangement gives larger reductions in all performance indexes. Although the level of differential displacements along the height is increased when compared to other configurations, the maximum, corresponding to that of the top floor, is smaller than that from either the UDD or the MIP (Figure 6.c). It is also worth noting that the averaged differential displacements are smaller than those corresponding to the static wind load that was used as a reference. As noted, incorporating the IDS is shown to result in a large improvement in the response under the far-field seismic records, with the SSSA spring placement method outperforming the other four distributions. The averaged results over the seven records and different performance indexes are included in Table 5.

Near-field records

While conventional TMDs have difficulties controlling the response of near-field excitations due to their inability to reach a resonant response condition, the IDS concept is able to mobilise a large mass ratio which mitigates this effect. Figure 7 depicts the top displacement time history

under the RSN764 record for all the spring distributions and the corresponding rigid case. The peak displacement is significantly reduced irrespective of the spring distribution deployed when compared with the rigid counterpart. The reduction is nearly the same level as for the far-field records (39%) with an average of 38% reduction (Table 5).

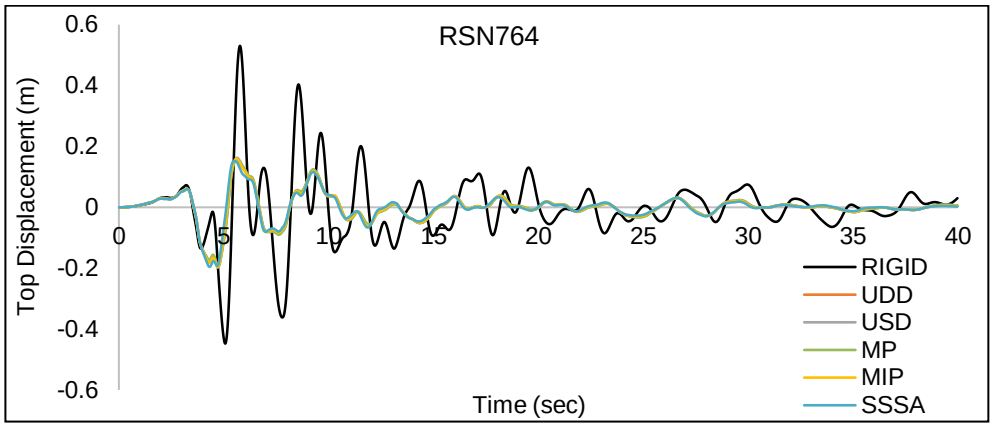

Figure 7: Top displacement for the RSN764 record for all spring distributions and the rigid case

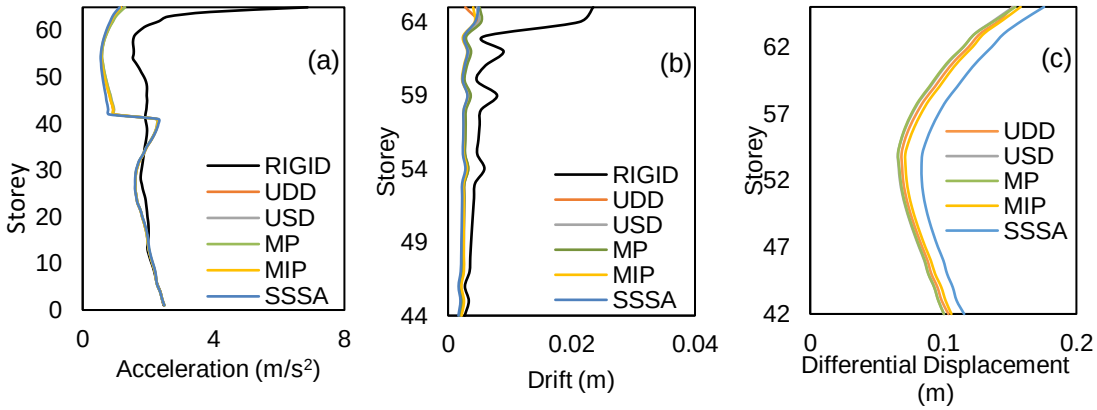

Figure 8: Averaged maximum absolute accelerations (a), averaged maximum inter-storey drifts (b), average maximum differential displacements (c) for near-field seismic records per floor

As shown in Figure 8.a, the absolute accelerations averaged over the seven records are reduced when compared to the fixed case. However, it is worth noting that the reduction is smaller than that for the far field records and experiences a peak at the point of transition between the IDS and the conventional floors. This occurs when considering large mass TMDs (Shariatmadar and Razavi, 2010). The inter-storey drifts are highly reduced when compared to the rigid counterpart and especially at the top floors (Figure 8.b). In a similar manner to that of the far-field case, it is the SSSA distributions provide the best performance, although all arrangements offer satisfactory responses.

The differential displacements between the movable floors and the core are reported in Figure 8.c. The SSSA arrangement results in slightly larger displacements than the other four distributions, which, following the same profile, behave relatively similarly, with the USD and MP giving smaller displacements. Averaged performance indexes over the building height and over the seven records are reported in Table 5 for both far and near-field cases. From the results, it is clear that the system performs slightly better for the far-field records than for the near-field case. The top displacement was reduced by 37-43% for the far-field, while the corresponding value for near-field ranged within 38-39%. Absolute accelerations reduction through the whole height for the far-field records was between 39% to 41%, compared to 25% to 26% for the near-field. The inter-storey drifts also reduced by 35%-39% for the far-field and 32%-35% for the near-field. It is also worth noting that the resulting averaged differential displacements for both sets of records are below the static wind loading. Although this will vary depending on the site seismicity and wind speed, considering that the stating wind load as an initial reference seems to provide similar results when subjected to real seismic excitations.

Response parameter	UDD	USD	MP	MIP	SSSA
Far-Field					
Average top displacement reduction	38%	38%	37%	39%	43%
Average drift reduction through the whole building height	35%	37%	36%	39%	39%
Average absolute acceleration reduction through the whole building height	39%	39%	39%	39%	41%
Average differential displacement (mm)	93	91	91	96	109
Near-Field					
Average top displacement reduction	38%	38%	38%	38%	39%
Average drift reduction through the whole building height	33%	33%	32%	34%	35%
Average absolute acceleration reduction through the whole building height	25%	25%	25%	25%	26%
Average differential displacement (mm)	93	90	90	96	108

Table 5: Performance indexes averaged over all stories, for near-field and far-field records

Pulse-like records

The results for the pulse-like records are reported herein only for the USD spring arrangement for the purpose of brevity and since it is the most conventional case. Results for other distributions followed a similar pattern as that shown for the near-field set. Even though TMDs are ineffective when dealing with pulse-like excitations, and while the IDS did not provide a substantial response reduction as that shown for all performance indexes for the far-field records under the SSSA distribution, it still resulted in a significant improvement. The reduction in the four considered performance indexes for each of the considered sets of records under the USD distribution is given in Table 6. As indicated, the IDS enhanced the response notably when compared to the fixed counterpart. The top displacements were reduced by 29%, drifts by 33%, and accelerations by 21%. These values are slightly smaller than those for other record sets, yet still offer significant advantages and illustrate the IDS capability in overcoming the limitations of conventional TMDs when dealing with near-field or pulse-like excitations.

Response parameter	Far-field (USD)	Near-field (USD)	Pulse-like (USD)
Average top displacement reduction	38%	38%	29%
Average drift reduction through the whole building height	37%	33%	33%
Average absolute acceleration reduction through the whole building height	39%	25%	21%
Average differential displacement (mm)	91	90	90

Table 6: Performance indexes averaged over all stories for the USD spring distribution

Conclusions

The paper investigated the seismic response of the novel integrated damping system (IDS), with a focus on the influence of the springs characteristics and arrangement. The system mobilises a large part of the building as a damper mass and connects it to the main frame via a series of springs and fluid viscous dampers in parallel. The springs play a critical role in the response as they define the level of differential displacement that can occur between the core and the movable mass. The study assessed the seismic response under suites of near-field, far-field, and pulse-like strong motion records. The assessments were performed with five spring arrangements, namely, Uniform Differential Displacement (UDD), Uniform Spring Distribution (USD), Modal Proportional (MP), Modal Inverted Proportional (MIP), and Simplified Sequential Search Algorithm (SSSA).

The results showed that the IDS system performed best for far-field records, which can engage a resonant response, yet was still able to achieve substantial improvements in both the near-field and pulse-like- situations. Average reductions in top displacement ranged from 29% to 43%, drifts from 3% to 39%, and accelerations from 21 to 41%. The level of differential displacement between the movable mass and core was kept below wind static displacements ranging from 90 mm to 109 mm. Although not as simple as the UDD or USD, the SSSA stiffness distribution was shown to outperform the other four distributions partly due to its higher overall flexibility, generating up to 7.5% first mode additional damping, followed by the MIP. Nonetheless, the response using other arrangements, such as the USD was also shown to be within the same order of magnitude and hence can also be effectively employed based on higher practicality. Moreover, the IDS approach was able to overcome the well-known deficiency of conventional TMDs when dealing with pulse excitations. The pulse-like set led to a smaller reduction in response when compared to the far or near-field records, yet still achieved a substantial improvement that can significantly reduce the structural demands and allow considerable efficiencies in the design of tall buildings.

References

Bravo, Liapopoulou and Elghazouli, (2020) Seismic collapse capacity assessment of SDOF systems incorporating duration and instability effects. Doi: 10.1007/s10518-020-00829-9

Chang, K.C. et al. (1995) 'Seismic Behaviour of Steel Frame with Added Viscoelastic Dampers', Journal of Structural Engineering, 121(10), Doi: 10.1061/(ASCE)0733-9445(1995)121:10(1418).

Cheng, Y. and Bai, G.L. (2017) 'Basic characteristic parameters and influencing factors of long-period ground motion records', Journal of Vibroengineering. Doi: 10.21595/jve.2017.18006.

Connor, J.J. (2003) Introduction to Structural Motion Control. Prentice Hall Pearson Education, Incorporated.

Constantinou, M.C. and Symans, M.D. (1993) 'Experimental study of seismic response of buildings with supplemental fluid dampers', The Structural Design of Tall Buildings, 2(2), pp. 93–132. Doi: 10.1002/tal.4320020203.

Cuka R. (2022) Parametric analyses on spring distribution arrangements when incorporating the integrated damping system, MSc Dissertation. Imperial London College, United Kingdom

Gutierrez Soto, M. and Adeli, H. (2013) 'Tuned Mass Dampers', Archives of Computational Methods in Engineering, 20(4), pp. 419–431. Doi: 10.1007/s11831-013-9091-7.

Jackson, M. and Scott, D.M. (2012) 'Increasing Efficiency in Tall Buildings by Damping', pp. 3132–3142, Structures Congress 2010, Florida, USA. Doi: 10.1061/41130(369)281.

Lopez Garcia, A Simple Method for the Design of Optimal Damper Configurations in MDOF Structures Earthquake. Spectra 2001, 17(3), 387. Doi: 10.1193/1.1586180

Martinez-Paneda, M. and Elghazouli, A.Y. (2020) 'An integrated damping system for tall buildings', The Structural Design of Tall and Special Buildings, 29(7), p. e1724. Doi: 10.1002/tal.1724.

Martinez-Paneda, M. and Elghazouli, A. Y. (2021) "Optimal Application of Fluid Viscous Dampers in Tall Buildings Incorporating Integrated Damping Systems", The Structural Design of Tall and Special Buildings, 30(17), e1892, Doi: 10.1002/tal.1892

Martinez-Paneda, M. and Elghazouli, A.Y. (2022) 'Seismic Performance of tall buildings with novel damping approaches', 3rd European Conference on Earthquake Engineering & Seismology Bucharest, Romania,2022

Matta, E. and De Stefano, A. (2009) 'Seismic performance of pendulum and translational roof-garden TMDs', Mechanical Systems and Signal Processing. Doi: 10.1016/j.ymssp.2008.07.007.

Pall, A.S. and Marsh, C. (1982) 'Response of Friction Damped Braced Frames', Journal of the Structural Division, 108(6), pp. 1313–1323. Doi: 10.1061/JSDEAG.0005968.

Papagiannopoulos, G. and Hatzigeorgiou, G. (2011) 'On the use of the half-power bandwidth method to estimate damping in building structures', Soil Dynamics and Earthquake Engineering - SOIL DYNAM EARTHQUAKE ENG, 31, pp. 1075–1079. Doi: 10.1016/j.soildyn.2011.02.007.

Perry, C.L. et al. (1993) 'Seismic Upgrade in San Francisco Using Energy Dissipation Devices', Earthquake Spectra, 9(3), pp. 559–579. Available at: Doi: 10.1193/1.1585730.

Rana, R. and Soong, T.T. (1998) 'Parametric study and simplified design of tuned mass dampers', Engineering Structures, 20(3), pp. 193–204. Doi: 10.1016/S0141-0296(97)00078-3.

Shariatmadar, H. and Razavi, H. (2010) 'Multi-Tuned Mass Dampers for Seismic Response Reduction of Mid and High-Rise Buildings' 5th National Congress on Civil Engineering, Ferdowsi University of Mashhad, Iran, 2010

Smith, R.J. and Willford, M.R. (2007) 'The damped outrigger concept for tall buildings', The Structural Design of Tall and Special Buildings, 16(4), pp. 501–517. Doi: 10.1002/tal.413.

Soong, T.T. and Spencer, B.F. (2002) 'Supplemental energy dissipation: state-of-the-art and state-of-the-practice', Engineering Structures, 24(3), pp. 243–259. Doi: 10.1016/S0141-0296(01)00092-X.

Xu, K. and Igusa, T. (1992) 'Dynamic characteristics of multiple substructures with closely spaced frequencies', Earthquake Engineering & Structural Dynamics. Doi: 10.1002/eqe.4290211203.